

## STRUCTURAL PERFECTION OF $\text{Hg}_{1-x}\text{Cd}_x\text{Te}$ GROWN BY THM

C. GENZEL, P. GILLE, I. HÄHNERT, F.M. KIESSLING and P. RUDOLPH

*Bereich Kristallographie, Sektion Physik der Humboldt-Universität Invalidenstrasse 110, DDR-1040 Berlin, German Dem. Rep.*

The defect structure of single crystals of  $\text{Hg}_{1-x}\text{Cd}_x\text{Te}$  grown by the travelling heater method (THM) has been investigated using X-ray double crystal topography and a chemical etching technique. The structural perfection is found to depend on the ratio of growth and solidus temperature  $T_g/T_s$ .

### 1. Introduction

The travelling heater method has proved successful for growing  $\text{Hg}_{1-x}\text{Cd}_x\text{Te}$  single crystals of both axially and radially high homogeneity [1]. In literature, growth conditions as well as electrical properties of the material have been investigated in a broad range, but there is a considerable lack in information on its structural perfection.

Especially in crystals with low Peierls stress such as the II–VI compounds the defect structure (dislocations, low-angle grain boundaries) is known to be very sensitive to variations of the growth parameters. Thus, investigations directed to this specific object may give information which is helpful to find optimum growth conditions as to improve the structural perfection. In this paper X-ray double crystal topography (DCT) and a chemical etching technique have been used to study the defect structure of THM-grown  $\text{Hg}_{1-x}\text{Cd}_x\text{Te}$  in dependence on the growth temperature. Both analytical methods complement one another quite efficiently; DCT is very sensitive to local and long-range lattice strain: by means of etching, the actual subgrain structure and high etch pit densities can be detected.

### 2. Experimental details

Crystals about 16 mm in diameter were grown from Te-rich solutions using source ingots obtained from quenched stoichiometric melts or from

a first THM process. Use was made of a simple one-zone furnace producing axial temperature gradients as high as  $85 \text{ K cm}^{-1}$  in the liquid adjacent to the phase boundary. When varying the temperature  $T_g$  at the growing interface by a variation of the furnace power, a different amount of tellurium was used to keep the zone length constant in all the runs to compare. Because of the strong increase of the liquidus and solidus temperature with an increasing mole fraction  $x$  in the  $\text{HgTe}$ – $\text{CdTe}$  system, the temperature of the growth from solution is reported in relation to the solidus temperature  $T_s$  of the same mole fraction. The growth conditions of the samples under investigation are summarized in table 1.

The ingots grown from  $(111)_A$ - or  $(\bar{1}\bar{1}\bar{1})_B$ -oriented  $\text{CdTe}$  seeds have always been single-crystalline as detected by X-ray reflection topographs. Contrary to the results obtained by Colombo et al. [2], we have not found remarkable differences with both directions.  $(111)$ -oriented samples with damage-free surfaces for reflection topography

Table 1  
Crystal growth temperatures

Sample	Mole fraction $x$	Growth temperature $T_g$ (K)	Solidus temperature $T_s^{a)}$ (K)	$T_g/T_s$
A	0.22	875	980	0.89
B	0.70	850	1122	0.76
C	0.22	803	980	0.82

<sup>a)</sup> After ref. [5].

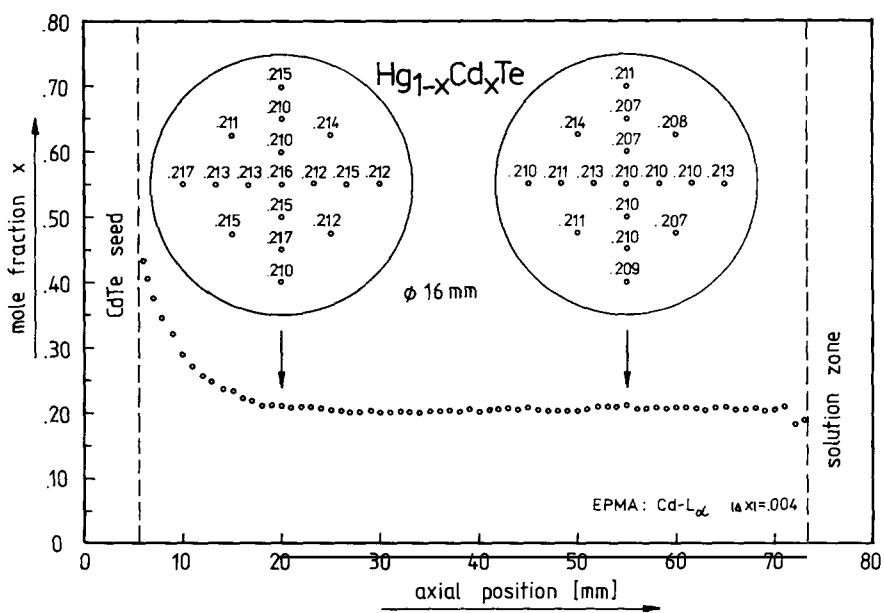


Fig. 1. Axial and radial plot of the mole fraction  $x$  of a typical  $Hg_{1-x}Cd_xTe$  ingot measured by electron microprobe.

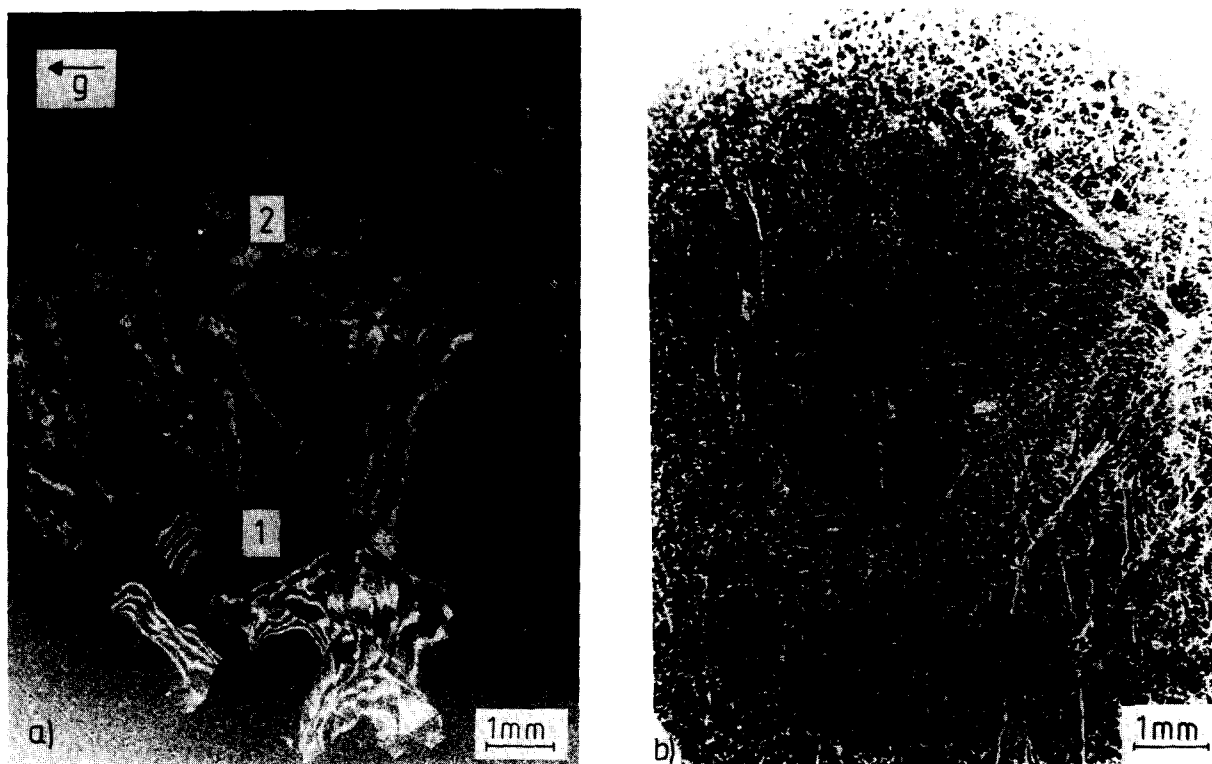


Fig. 2. (a) 531-topograph series of a  $Hg_{0.78}Cd_{0.22}Te$  specimen (sample A) taken successively at intervals of 60 arc sec: (1) area of strong local lattice strain; (2) subgrain structure superimposed by long-range lattice distortion. (b) Optical micrograph of the etched  $(111)_A$  surface of a  $Hg_{0.78}Cd_{0.22}Te$  specimen (sample A) showing the typical subgrain structure.

were prepared by a procedure including cutting, lapping, and mechanical and chemical polishing.

Metallurgical homogeneity was measured by means of electron probe microanalysis (EPMA) at a 17 point wafer scanning pattern. The crystals have a high axial ( $|\Delta x| \leq 0.004$ ) as well as radial ( $|\Delta x| \leq 0.003$ ) homogeneity which is next to the detection limit of EPMA (fig. 1).

For the X-ray investigations use was made of a double crystal arrangement near the  $(n, -n)$  position.  $(100)$  Si was employed as collimator crystal. For  $\text{Cu K}\alpha_1$  radiation the reflex pair Si-422/MCT-531 corresponds. In this case a residual dispersion of 1 arc sec ensues. After topography, the samples were chemically etched using a newly developed etchant [3].

### 3. Results and discussion

Fig. 2 shows the typical defect structure in THM-grown material (sample A) for a high ratio of  $T_g/T_s$ . It consists of a low-angle subgrain structure with grains of 50 up to about 300  $\mu\text{m}$  misoriented by 60 to 120 arc sec. By means of superposition topographs taken successively at intervals of 60 arc sec (fig. 2a), the subgrain structure can be shown to be superimposed by long-range distortions as well as by strong local lattice strain due to non-linear and high temperature gradients during growth. Local variations of the lattice parameter giving rise to an additional contrast within the topograph have been excluded by measuring the angular positions of a symmetrical diffraction peak at two incident azimuths making  $180^\circ$  to each other [4]. Thus, the X-ray investigations are in agreement with the results obtained by EPMA showing the high metallurgical homogeneity of the material considered. The dislocation density is too high for resolving individual dislocations. Subgrains are only visible in weakly deformed regions.

Information on the actual size of subgrains and both density and distribution of dislocations is obtained by etching (fig. 2b). The EPD is about  $3 \times 10^5 \text{ cm}^{-2}$ . What is striking is its increase near the edges of the sample ( $\text{EPD} > 10^6 \text{ cm}^{-2}$ ) connected with a decreasing size of the subgrains. This effect, which has also been detected by means



Fig. 3. 531-topograph of a  $\text{Hg}_{0.3}\text{Cd}_{0.7}\text{Te}$  specimen (sample B) showing large grains at the centre and a subgrain structure at the edge of the slice.

of topography for samples of higher structural perfection (fig. 3), is supposed to be caused by the contact between silica ampoule and crystal.

A considerable improvement of the structural perfection can be achieved by a lower ratio of  $T_g/T_s$  which can be varied in solution growth in a broad range. In this case, as shown in the topographs in figs. 3 and 4a, the subgrain structure consists of large grains up to a size of about  $1 \text{ mm}^2$ . The misorientation between the grains is lower than 30 arc sec. Strong long-range lattice deformations are not in evidence. The dislocation density is lower than  $10^5 \text{ cm}^{-2}$ . This offers the possibility to compare the defect structure observed in X-ray topograph and etch pit pattern of the surface with respect to both nature and distribution of individual defects.

Thus, fig. 4 shows the excellent agreement of dislocation and etch pit distribution in topograph

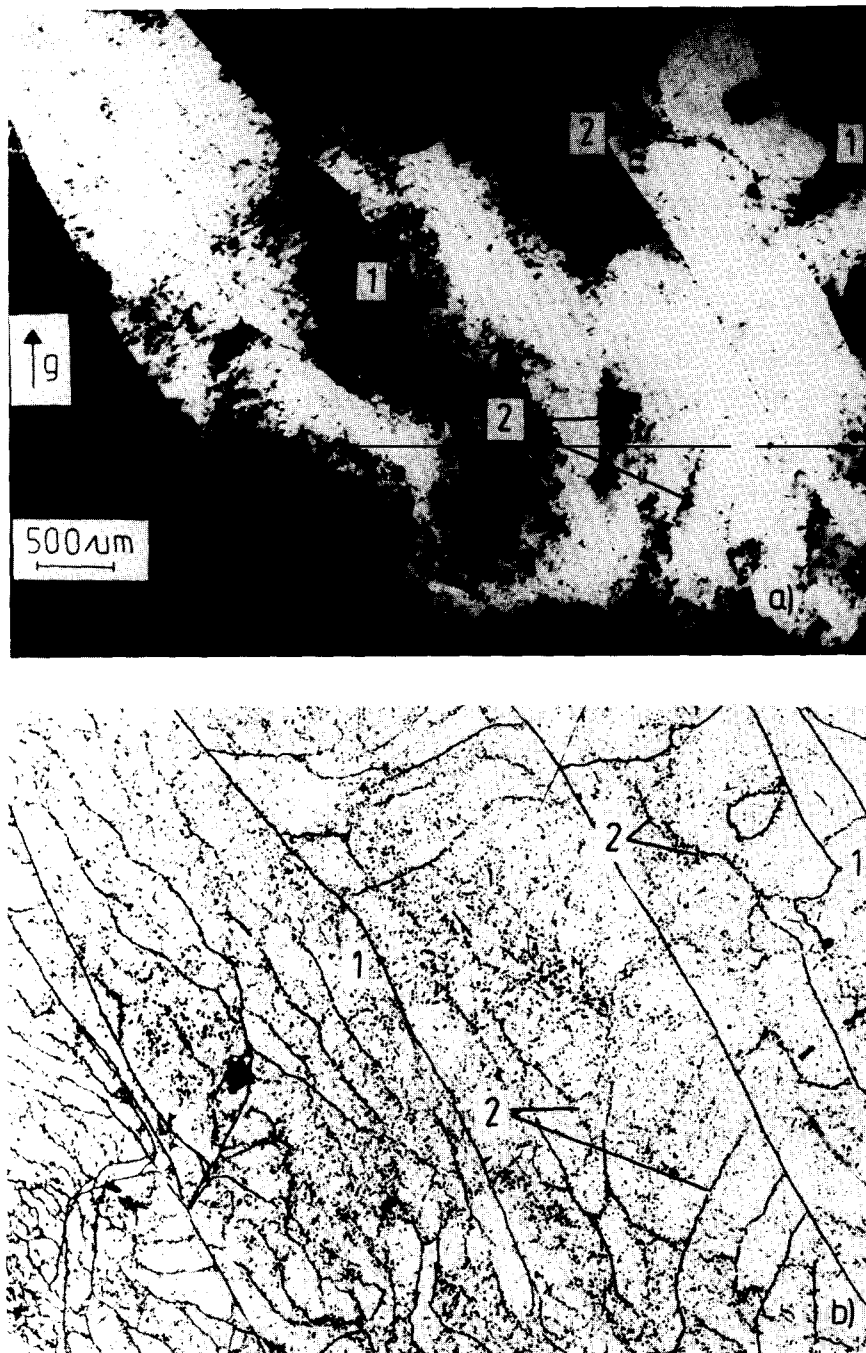


Fig. 4. Comparison of (a) 531-topograph and (b) etch pit micrograph of a  $\text{Hg}_{0.78}\text{Cd}_{0.22}\text{Te}$  specimen (sample C) showing excellent agreement in details of the defect structure: (1) low-angle grain boundary; (2) dislocations forming low-angle grain boundaries by means of polygonization.

and micrograph, respectively, which is best to be seen in low-angle grain boundaries. Due to the invisibility of such dislocations for which  $\mathbf{g} \cdot \mathbf{b} \approx 0$  ( $\mathbf{g}$  = diffraction vector,  $\mathbf{b}$  = Burgers vector), the etch pit density is about 1.5 up to 2.0 times higher than the dislocation density detected by one topograph. Dislocations parallel to the surface are only to be seen in the topograph. Most of them run into the  $\langle 110 \rangle$  directions. In special cases dislocations can be observed to form low-angle grain boundaries by means of polygonization; topograph as well as micrograph show the spreading of the dislocations around the subgrain boundaries which are in the process of development. The misorientation of the adjacent regions is only a few arc sec.

It is well known that non-linear and high temperature gradients during growth affect the perfection of the crystals grown. They generate dislocations which can move and form low-angle grain boundaries. Therefore, it should be desirable to establish a smooth temperature field in the crystal next to the solid/liquid interface with only low temperature gradients.

Contrary to that, crystal growth by THM inevitably needs very high axial temperature gradients in order to provide the material and heat transport. Effects of thermoelastic stress can be decreased by lowering the absolute temperatures as we did, but probably there exists a limit of structural perfection of THM-grown  $\text{Hg}_{1-x}\text{Cd}_x\text{Te}$  crystals that cannot be overcome.

#### 4. Conclusions

$\text{Hg}_{1-x}\text{Cd}_x\text{Te}$  single crystals were grown by the travelling heater method applying different tem-

peratures of growth. It has been found by means of X-ray double crystal topography and a chemical etching technique that results obtained with the two methods show an excellent agreement of dislocation and etch pit distributions. The structural perfection of THM-grown crystals strongly depends on the conditions used. Crystal growth temperatures with  $\text{Hg}_{1-x}\text{Cd}_x\text{Te}$  of different mole fractions  $x$  should be compared with respect to the solidus temperature of the crystal to grow. With interface temperatures as low as  $530^\circ\text{C}$  for  $x = 0.22$ , dislocation densities lower than  $10^5\text{ cm}^{-2}$  and subgrain structures with grains of about  $1\text{ mm}^2$  misoriented by less than 30 arc sec could be obtained.

#### Acknowledgement

The authors are grateful to Mr. M. Burkert for carrying out the electron probe microanalysis measurements.

#### References

- [1] R. Triboulet, T. Nguyen Duy and A. Durand, *J. Vacuum Sci. Technol.* A3 (1985) 95.
- [2] L. Colombo, R.R. Chang, C.J. Chang and B.A. Baird, *J. Vacuum Sci. Technol.* A6 (1988) 2795.
- [3] I. Hähnert and M. Schenk, *J. Crystal Growth* 101 (1990) 251.
- [4] S. Kikuta and K. Kohra, *Japan. J. Appl. Phys.* 5 (1966) 1047.
- [5] J.C. Brice, *Progr. Crystal Growth Characterization* 13 (1986) 39.